Macromolecular Research, Vol. 22, No. 10, pp 1059-1065 (2014)
DOI 10.1007/s13233-014-2157-z

www.springer.com/13233
pISSN 1598-5032 eISSN 2092-7673

Microstructure and Electrical Property of Epoxy/Graphene/MWCNT Hybrid Composite Films Manufactured by UV-Curing

Young Gyu Jeong*,[1] and Ji-Eun An[2]

[1]*Department of Advanced Organic Materials and Textile System Engineering, Chungnam National University, Daejeon 305-764, Korea*
[2]*New Business Team, H&SHighTech Corp., 62-7, Techno 1-ro, Yuseong-gu, Daejeon 305-509, Korea*

Received March 11, 2014; Revised June 24, 2014; Accepted July 12, 2014

Abstract: UV-cured epoxy hybrid composite films were manufactured by efficient and facile cationic photochemical polymerization of 3,4-epoxycyclohexylmethyl-3',4'-epoxycyclohexane carboxylate mixtures including 5.0 wt% carbon nanofillers of different graphene/multi-walled carbon nanotube (MWCNT) compositions of 10/0, 9/1, 7/3, 5/5, 3/7, and 0/10 by weight ratio. TEM images confirmed that the mixed carbon nanofillers of graphene and MWCNT were well dispersed in the UV-cured epoxy matrix, while MWCNT as a single carbon nanofiller component was aggregated in the matrix. The electrical resistivity of the composite films was thus varied with the increment of the relative MWCNT content in 5.0 wt% carbon nanofillers, *i.e.*, ~160 Ωcm for the epoxy/graphene composite film, 30~80 Ωcm for the epoxy/graphene/MWCNT composite films, and ~16,200 Ωcm for the epoxy/MWCNT composite film. The decreased electrical resistivity of the epoxy/graphene/MWCNT composite films was associated with the interconnected network formation of graphene sheets and MWCNTs. Thus the UV-cured epoxy/graphene and epoxy/graphene/MWCNT composite films exhibited excellent electric heating performance in terms of rapid temperature response, stable maximum temperature, and high electric power efficiency. In addition, the UV-cured epoxy hybrid composite films as electric heating materials were found to be thermally stable up to ~290 ºC.

Keywords: carbon nanotube, composite film, epoxy, graphene, microstructure, electrical property, UV-curing.

Introduction

Epoxy resins are known to be an important class of thermally or photochemically cross-linked polymers with excellent performance in adhesion, strength/stiffness, chemical/thermal/dimensional stability and creep/solvent resistance.[1,2] Owing to their excellent physic-chemical properties, in combination with the easy processibility and reasonable cost, epoxy resins have been extensively used for multi-purpose applications such as sealants, metal coatings, electronics/electrical components, composite matrix, textile finishing and structural adhesives.[3] Especially, UV-assisted photochemical curing technique of epoxy compounds has gained increasing importance in the field of coatings and films due to its peculiar characteristics of single epoxy component, solvent-free and low-temperature process.[4] Among various photochemical curing techniques, the cationic ring-opening polymerization of epoxy compounds by UV-irradiation present additional advantages including lack of inhibition of oxygen, low shrinkage, good adhesion and mechanical properties, compared to the photochemically-induced radical polymerization.[5-7]

*Corresponding Author. E-mail: ygjeong@cnu.ac.kr

Recently considerable efforts have been devoted to yield epoxy-based hybrid materials with unique and multi-functional properties by introducing nanoscale particles to epoxy resins.[8-11] Especially, the inclusion of carbon-based nanofillers such as carbon nanotubes (CNTs),[12-16] carbon nanofibers,[17-21] graphene/graphite nanoplatelets,[22-26] and carbon blacks,[27-30] into insulating epoxy resins have allowed to obtain electrically conductive epoxy nanocomposites. Recently, epoxy composites including mixed or hybrid carbon nanofillers of two-dimensional graphene sheets and one-dimensional CNTs have been also manufactured.[31-35] It was investigated that the mixed or hybrid carbon nanofillers composed of graphene sheets and CNTs could be more effectively dispersed in the epoxy matrix, and they could contribute more highly to enhance mechanical property and thermal/electrical conductivity, compared with single-component carbon nanofillers. The epoxy nanocomposites reinforced with carbon nanofillers can be applied for electromagnetic shielding, electronic components, capacitors, electrodes for rechargeable batteries, sensors, actuators, and electric heating elements.

In the current study, a series of epoxy-based hybrid composite films reinforced with 5.0 wt% carbon nanofillers were manufactured by simple and efficient UV-curing technique.

3,4-Epoxycyclohexylmethyl-3',4'-epoxycyclohexane carboxylate and triarylsulfonium hexafluoroantimonate salts were used as the epoxy compound and initiators for the cationic ring-opening polymerization by UV-irradiation, respectively, The 5.0 wt% carbon nanofillers as reinforcing components were composed of graphene sheets and multi-walled carbon nanotubes (MWCNTs) (graphene/MWCNT=10/0, 9/1, 7/3, 5/5, 7/7, and 0/10 by weight ratio). For the UV-cured epoxy hybrid composite films, the microstructure and electrical resistivity were characterized as a function of the graphene/MWCNT ratios in 5.0 wt% carbon nanofillers. The electric heating performance of the hybrid composite films was then analyzed by taking into account the temperature response rapidity and electric power efficiency at different applied voltages. The thermal stability of the hybrid composite films was also examined and discussed.

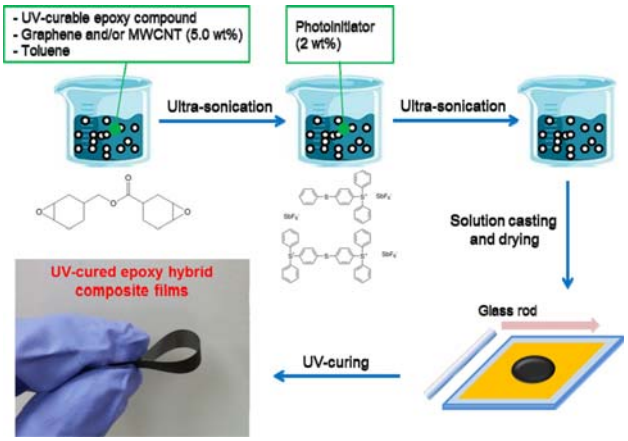

Figure 1. Schematic procedure for manufacturing UV-cured epoxy hybrid composite films with 5.0 wt% carbon nanofillers of different graphene/MWCNT compositions.

Experimental

Materials. 3,4-Epoxycyclohexylmethyl-3',4'-epoxycyclohexane carboxylate (Sigma-Aldrich Inc.) was used as an epoxy compound and triarylsulfonium hexafluoroantimonate salt (Sigma-Aldrich Inc.) was as a photoinitiator of UV-curing. MWCNTs (CM-250, Hanwha Chemical Co., Inc) with average diameter of 10~15 nm and length of ~100 μm were used as 1-dimensional carbon nanofillers. Natural graphite (flake type, Sigma-Aldrich Inc.) with an average diameter of ~500 μm was used for preparing conductive graphene sheets via an oxidation and rapid thermal expansion technique. Sulfuric acid (95%, Junsei Chemical Co., Ltd.) and nitric acid (60%, Junsei Chemical Co., Ltd), and potassium chlorate (99.5%, Kanto Chemical Co., Inc.) are used for the oxidation of the natural graphite. The preparation and characterization of the graphene sheets as 2-dimensional carbon nanofillers was prepared by acid-treatment and following rapid thermal expansion of natural graphite flakes.[26,36-38] Firstly, a mixture of sulfuric acid (320 mL) and nitric acid (180 mL) was stirred in a round-bottom flask, which was cooled in an ice bath for 30 min. Natural graphite flakes (20 g) was added into the mixture and then stirred for 20 min. Potassium chlorate (220 g) was slowly added into the flask in the ice bath. The oxidation of natural graphite flakes was carried out for 120 h. After the oxidation, the mixture was washed with distilled water and filtered, which was repeated until neutral pH. The graphite oxide filtrates were dried in a vacuum oven at room temperature for 24 h. Finally, the exfoliated graphene sheets was obtained by the thermal expansion of the graphite oxide flakes at 1050 ºC for 30 s.

Preparation of UV-Cured Epoxy Hybrid Composite Films. UV-cured epoxy hybrid composite films containing 5.0 wt% carbon nanofillers of different graphene/MWCNT ratios were prepared by UV-curing techniques, as presented in Figure 1. Firstly, liquid mixtures of 3,4-epoxy cyclohexylmethyl-3',4'-epoxycyclohexane carboxylate with 5.0 wt% carbon nanofillers and toluene were ultrasonically agitated by using a horn-type sonicator (VC-505, Sonics & Materials, Inc.) for 20 min. The toluene solvent was added to lower the viscosity of the epoxy/carbon nanofiller mixtures and its amount was controlled to be 5.0 wt%. The photoinitiator, triarylsulfonium hexafluoroantimonate salt, was then added in the mixtures. The weight fraction of the photoinitiator to the epoxy compound was adjusted to be 2.0 wt%. The mixtures of epoxy/carbon nanofiller/photoinitiator were sonicated for 5 min and were applied on a commercially available polyimide film. Finally, the films were dried at 80 ºC for 4 h to remove the residual toluene solvent. Then, the epoxy/carbon nanofiller films were cured on a plate at 100 ºC for 1 h under UV-B irradiation with ~40 mW/cm^2 intensity at the sample position. The thickness in the UV-cured epoxy hybrid composite films was controlled to be ~100 μm. The final UV-cured epoxy hybrid composite films were coded as E/G, E/M, and E/G/M-x/y, where x and y denote the relative ratios of graphene and MWCNT in 5.0 wt% carbon nanofillers, respectively, as listed in Table I.

Table I. Sample Codes Corresponding to the Composition of the UV-Cured Epoxy Hybrid Composite Films Containing 5.0 wt% Carbon Nanofillers of Different Graphene/MWCNT Amounts

Sample Code	Epoxy Resin (wt%)	Carbon Nanofiller Composition	
		Graphene (wt%)	MWCNT (wt%)
E/G	95.0	5.0	0.0
E/G/M-9/1	95.0	4.5	0.5
E/G/M-7/3	95.0	3.5	1.5
E/G/M-5/5	95.0	2.5	2.5
E/G/M-3/7	95.0	1.5	3.5
E/M	95.0	0.0	5.0

Characterization. The structural order of the UV-cured epoxy hybrid composite films with 5.0 wt% carbon nanofillers of different graphene/MWCNT compositions was examined by using an X-ray Diffractometer (X-MAX/2000-PC, Rigaku) with Ni-filtered CuK_α radiation (40 kV and 150 mA), which was operated at the rate of 2°/min in the 2θ range of 3~50°. The dispersion state of the carbon nanofillers in the composite films was characterized with aid of a transmission electron microscope (TEM, JEM 2100, JEOL Ltd.). For TEM experiments, thin samples of ~80 nm thickness for all the composite films were prepared by using a cryo-ultramicrotome (PT-PC and CR-X, RMC). Thermal degradation behavior of the composite films was characterized by using a thermogravimetric analyzer (TGA, TA Q100) under the nitrogen gas condition at a heating rate of 10 °C/min. The electrical resistance and voltage-dependent current and electric power for the composite films were measured by employing multiple sourcemeters and ohmmeters (6517A, 2400, 2182A, Keithley Instruments Inc.). Electric heating behavior of the hybrid composite films at different applied voltages of 1~40 V were characterized with an Infrared camera (SE/A325, FLIR Systems Inc.) and a sourcemeter (2400, Keithley Instruments Inc.). For electrical property measurements, the composite films were cut to be 5.0 mm width and 20.0 mm length and the distance between two electrical probes was 10.0 mm.

Results and Discussion

Structural Characterization. In order to identify the structural order and packing state of the carbon nanofillers in the UV-cured epoxy matrix, X-ray diffraction patterns of exfoliated graphene, MWCNT, hybrid composite films with 5.0 wt% carbon nanofillers of different graphene/MWCNT compositions are obtained, as shown in Figure 2(A). For the neat MWCNT, a broad X-ray diffraction peak was detected at 2θ~26.4°, which corresponds to the *d*-spacing of 0.337 nm. This peak is caused by the cylindrically well layered structure of the pristine MWCNTs. Figure 2(B) shows the SEM image of the pristine MWCNT used in this study. On the other hand, exfoliated graphene sheets do not show any diffraction peak. It demonstrates that fully exfoliated graphene sheets were successfully obtained by the oxidation of the natural graphite and following rapid thermal expansion of the graphite oxide flakes, which can be confirmed by the SEM image shown in Figure 2(C). X-Ray diffraction patterns of the UV-cured epoxy hybrid composite films containing 5.0 wt% carbon nanofillers show only broad amorphous hallo scattering without any sharp diffraction peak associated with ordered crystalline structures of MWCNT and graphite. These results demonstrate that the carbon nanofillers of different graphene/MWCNT compositions remain as their disordered and unpacking state in the UV-cured epoxy matrix.

The dispersion state of the carbon nanofillers in the UV-cured hybrid composite films was characterized by using

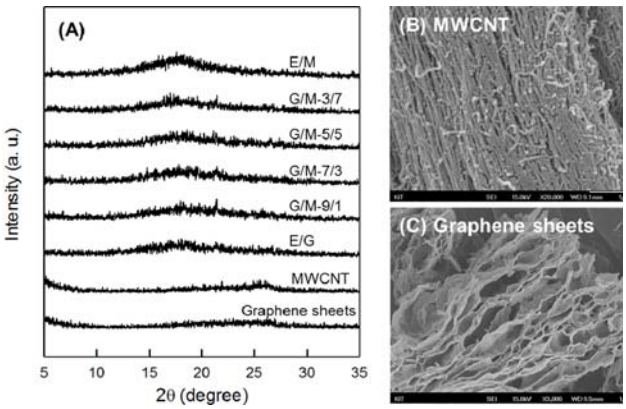

Figure 2. (A) X-Ray diffraction patterns of graphene sheets, MWCNT, and UV-cured epoxy hybrid composite films with 5.0 wt% carbon nanofillers of different graphene/MWCNT compositions and (B, C) SEM images of MWCNTs and graphene sheets used as carbon nanofillers.

TEM images of the cross-section of the hybrid composite films, as shown in Figure 3. In case of the E/G composite film, the graphene sheets are found to be well dispersed and percolated in the epoxy matrix (Figure 3(A)). On the other hand, for the E/M composite film, MWCNTs formed aggregated domains in the epoxy matrix (Figure 3(F)). In the cases of the E/G/M composite films, graphene sheets and MWCNTs were observed to be well dispersed by generating there interconnected networks in the epoxy matrix (Figure 3(B)~(E)). It was also found that the 2-dimensional graphene sheets are interconnected by the 1-dimensional MWCNTs, although the bridging effects become less effective for the hybrid composite films with higher MWCNT content in 5.0 wt% carbon nanofillers owing to the tendency to form MWCNT aggregates.

Thermal Stability. To characterize the thermal stability of the UV-cured epoxy hybrid composite films, TGA thermograms under the nitrogen gas condition were obtained, as shown in Figure 4. It was found that the weight loss of the composite films begins at ~290 °C. For a quantitative comparison, thermal degradation temperatures of 10% and 50% weight loss ($T_{10\%}$ and $T_{50\%}$) of the UV-cured composite films were evaluated and they were listed in Table II. It was characterized that the $T_{10\%}$ and $T_{50\%}$ values of the E/G composite film were 314.0 and 386.4 °C, respectively. In the case of the E/M composite film, the $T_{10\%}$ and $T_{50\%}$ values were 310.4 and 370.8 °C, which are 4 and 16 °C lower than those of the E/G composite film, respectively. For the E/G/M composite films, the $T_{50\%}$ value was found to decrease with the relative MWCNT content in 5.0 wt% carbon nanofillers, although the residue at 500 °C was slightly higher for the composite films with higher MWCNT content in the carbon nanofillers. It is thus considered that the higher thermal degradation temperature of the composite films with higher graphene content in 5.0 wt% carbon nanofillers originates from the barrier effect of 2-D graphene sheets to

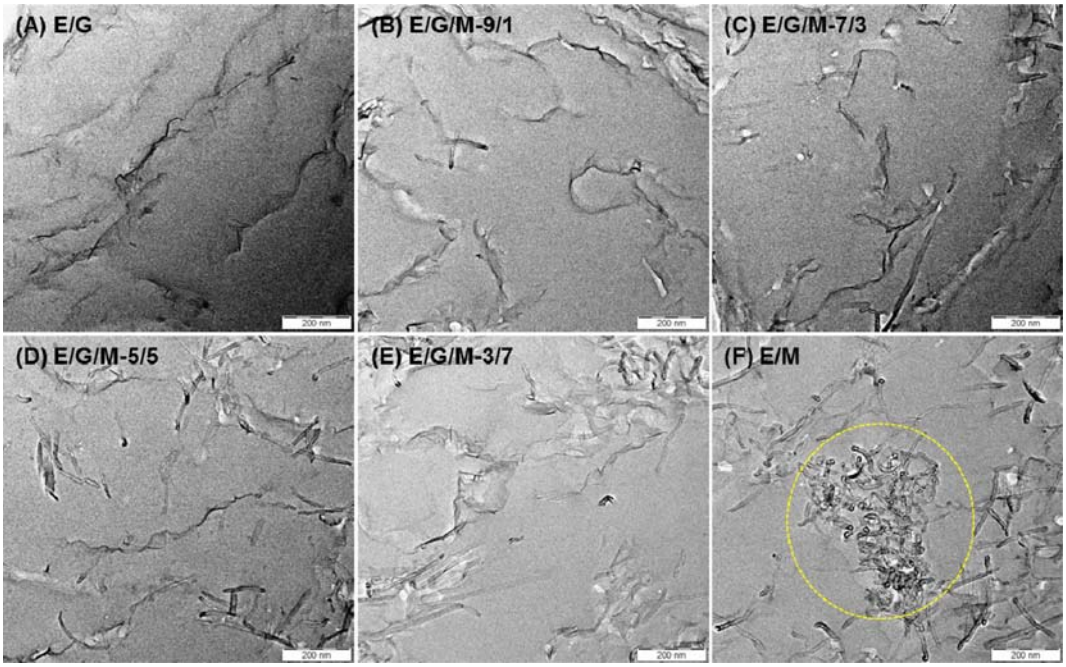

Figure 3. TEM images of cross-section of the UV-cured epoxy hybrid composite films with 5.0 wt% mixed carbon fillers of different graphene/MWCNT compositions.

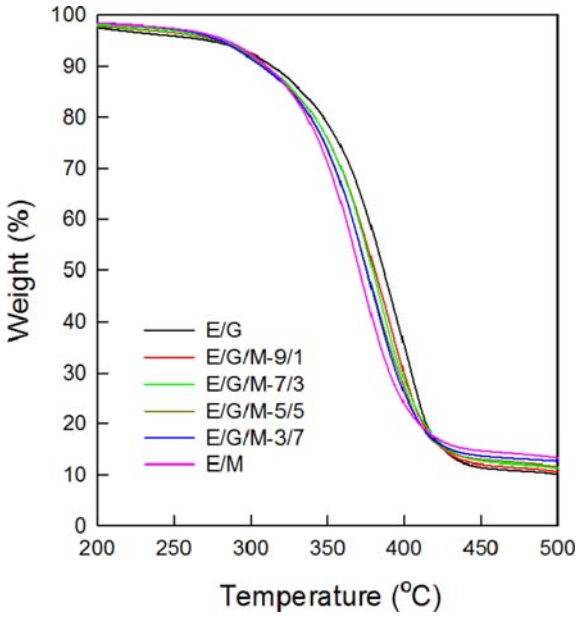

Figure 4. TGA thermograms of the UV-cured epoxy hybrid composite films with 5.0 wt% carbon nanofillers of different graphene/MWCNT compositions examined under the nitrogen gas condition.

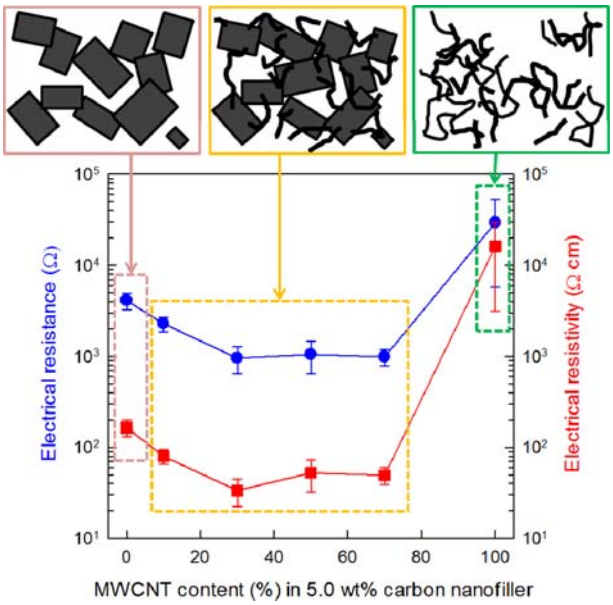

Figure 5. Electrical resistance and resistivity of the UV-cured epoxy hybrid composite films as a function of the relative content of MWCNT in 5.0 wt% carbon nanofillers.

the volatile low molecular compounds generated during the thermal decomposition of the UV-cured epoxy matrix. From the TGA results, it is expected that the UV-cured epoxy hybrid composites manufactured in this study can be used effectively as electric heating elements which do not require high maximum temperatures above 200 °C.

Electrical Properties. The electrical resistance and resistivity of the UV-cured epoxy hybrid composite films measured at an applied voltage of 1 V were presented as a function of the relative MWCNT content in 5.0 wt% carbon nanofillers, as can be seen in Figure 5. The electrical resistivity of the E/G composite film was measured to be ~160 Ωcm. On the other

hand, the resistivity of the E/M composite film was ~16,000 Ωcm owing to the MWCNT aggregation in the UV-cured epoxy matrix. In the cases of the E/G/M composite films, the electrical resistivity was in the range of 30~80 Ω cm, which was one to three orders of magnitude lower than those of the E/G and E/M composite films, respectively. This noticeably decreased electrical resistivity of the E/G/M composite films is believed to be associated with the increased conduction pathways due to the interconnected networks formed by 2-D graphene sheets and 1-D MWCNTs as discussed above. As the result, electric charges can flow more efficiently through the conduction paths of networked graphene sheets and MWCNTs in the E/G/M composite films.

The current-voltage (*I-V*) curves of the UV-cured epoxy hybrid composite films with different graphene/MWCNT compositions of 5.0 wt% carbon nanofillers are presented in Figure 6(A). For all the composite films, the electric current was increased linearly with the applied voltage and also the slopes of the *I-V* curves became steeper with increasing the relative MWCNT content of in 5.0 wt% carbon nanofillers. This linear *I-V* curves at the applied voltages up to ~25 V are related with the Ohm's law, which is expressed as $V=IR$ where V is the applied voltage, I is electrical current, and R is electrical resistance. It should note that the *I-V* curves of the E/G/M-7/3, E/G/M-5/5, and E/G/M-7/7 are almost identical within the experimental error, which results from their similar electrical resistances. On the other hand, it is considered that the slightly positive deviation from the linear *I-V* curves at higher applied voltages stems from the increment in the temperatures of the composite films owing to the electric heating behavior. Figure 6(B) displays the electric power-voltage (*P-V*) curves of the E/G, E/M, and E/G/M composite films. It was observed that the electric power of the composite films was quadratically proportional to the applied voltage, which was quite consistent with the relationship of $P=IV=I^2R$. Since the electric power is released as heat, the maximum temperatures of the UV-cured hybrid composite films attained at different applied voltages can be expected to be varied by the current as well as the electrical resistivity, as will be discussed below.

Electric Heating Performance. Electric heating, also called as Joule heating and resistive heating, is known to be caused by interactions between the moving particles (usually electrons) that form the current and the atomic ions that make up the conductive materials. Charged particles in an electric circuit are accelerated by an electric field but lose some of their kinetic energy by colliding with the atomic ions. The increment in the kinetic or vibrational energy of the atomic ions manifests itself as heat and a rise in the temperature of the conductive materials. In this way, the electrical energy from the electrical power supply is partially converted to the thermal energy of the conductive materials.

The electric heating performance of the UV-cured epoxy hybrid composite films with 5.0 wt% carbon nanofillers of different graphene/MWCNT compositions was investigated by measuring the temperature of the hybrid composite films as a function of time at different applied voltages of 1~25 V, as can be seen in Figure 7. For the E/G composite film, the temperature was not changed with time at the applied voltages of 1~5 V owing to its high electrical resistance (Figure 7(A)). When the higher voltages above 10 V were applied at ~8 s, maximum temperatures of the film were reached within ~20 s and remained constant over time. When the applied voltages were off at ~185 s, the film temperatures were decreased to

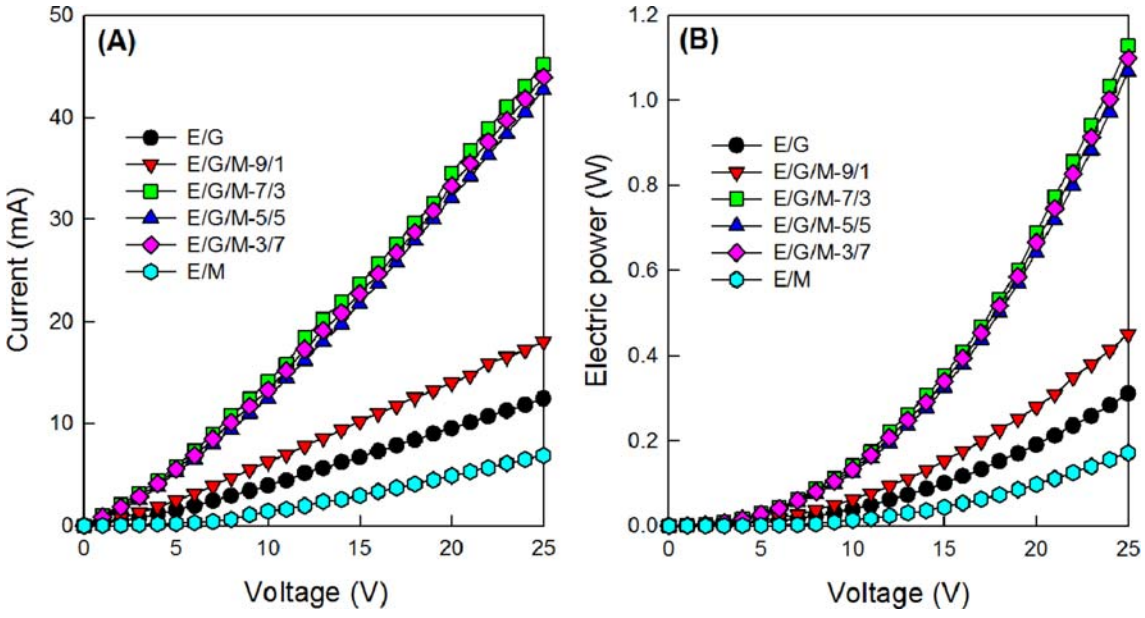

Figure 6. (A) current-voltage and (B) electric power-voltage curves of the UV-cured epoxy hybrid composite films with 5.0 wt% carbon nanofillers of different graphene/MWCNT compositions.

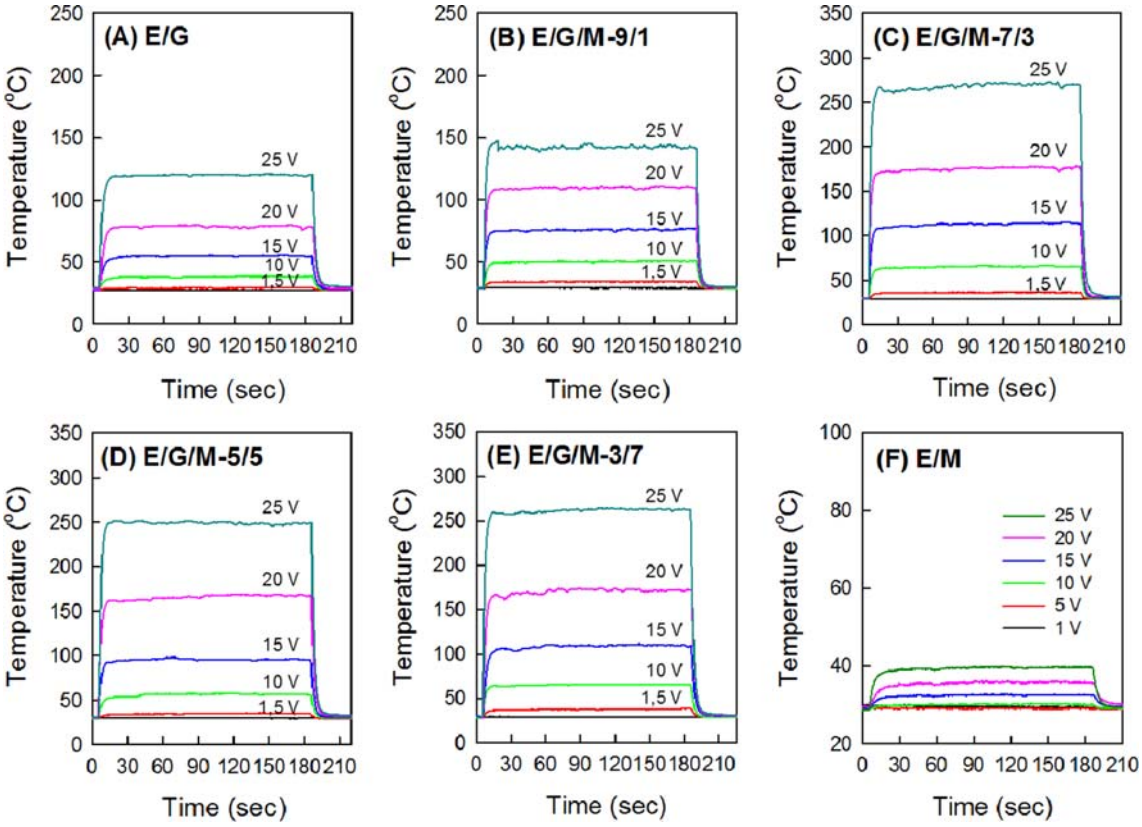

Figure 7. Time-dependent temperature changes at different applied voltages of 1~25 V for the UV-cured epoxy hybrid composite films with 5.0 wt% carbon nanofillers of different graphene/MWCNT compositions: (A) E/G; (B) E/G/M-9/1; (C) E/G/M-7/3; (D) E/G/M-5/5; (E) E/G/M-3/7; (F) E/M.

room temperature within ~20 s. This rapid temperature response to the applied voltages was also observed for other E/G/M composite films, although the maximum temperatures reached at different applied voltages were varied depending on the graphene/MWCNT compositions in 5.0 wt% carbon nanofillers (Figure 7(B)~(E)). On the other hand, it should be mentioned that there was only weak electrical heating performance for the E/M composite film (Figure 7(F)), which resulted from its high electrical resistance or low electric power due to the inhomogeneous dispersion of MWCNTs in the UV-cured epoxy matrix, as confirmed in Figures 3 and 6.

The electric heating efficiency of the UV-cured hybrid composite films was examined by evaluating the heat released during the maximum and equilibrium temperature region (8~185 s) of Figure 7(A)~(F). According to the conservation law of energy, the heat gain by electric power is supposed to be equal to the heat loss by radiation and convection. Accordingly, the heat transferred by radiation and convection, h_{r+c}, can be calculated by using the following equation:

$$h_{r+c} = \frac{I_c V_0}{T_m - T_0} \quad (1)$$

where I_c, V_0, T_0, and T_m are initial temperature, maximum temperature, steady-state current, and applied voltage, respectively. Using the data of Figures 6(A) and 7, the h_{r+c} values were calculated, as listed in Table II. It was found that the h_{r+c} values for the E/G and E/G/M composite films were in the range of 3.40~4.73 mW/°C, while the value for the E/M composite film was ~14.28 mW/°C. These results indicate that the UV-cured E/G and E/G/M composite films have excellent electric heating efficiency by requiring relatively low electrical energy to maintain stable maximum temperatures.

Table II. Characteristic Temperatures ($T_{10\%}$ and $T_{50\%}$) at 10% and 50% Weight Loss by Thermal Decomposition and Heat (h_{r+c}) Transferred by Radiation and Convection During Electric Heating for the UV-Cured Epoxy Hybrid Composite Films

Sample Code	$T_{10\%}$ (°C)	$T_{50\%}$ (°C)	h_{r+c} (mW/°C)
E/G	314.0	386.4	3.6±0.2
E/G/M-9/1	307.3	380.6	3.4±0.5
E/G/M-7/3	309.9	379.2	4.4±0.4
E/G/M-5/5	309.6	375.5	4.7±0.2
E/G/M-3/7	307.1	374.4	4.3±0.5
E/M	310.4	370.8	14.3±1.7

Conclusions

UV-cured epoxy hybrid composite films were manufactured by simple and efficient cationic ring opening-curing of an epoxy-based mixtures containing 5.0 wt% carbon nanofillers of different graphene/MWCNT compositions under UV light. The X-ray diffraction patterns and TEM images confirmed that the mixed graphene sheets and MWCNTs formed their interconnected network structure in the UV-cured E/G/M epoxy resin matrix, while the MWCNTs were aggregated in the E/M composite film. Accordingly, the electrical resistivity (30~80 Ωcm) of the E/G/M composite films was found to be lower than those (~160 and ~16,200 Ωcm) of the E/G and E/M composite films. The electric heating behavior of the composite films was thus strongly dependent on the applied voltage as well as the graphene/MWCNT composition. The E/G and E/G/M composite films with relative low electric resistivity exhibited rapid temperature response to the applied voltages of 5~25 V and their stable maximum temperatures were maintained depending on the applied voltage. It was also found that the UV-cured hybrid composite films were thermally stable up to ~290 °C. Overall, it is believed that the UV-cured epoxy hybrid composite films with excellent electric heating performance and high thermal stability can be applied as advanced electric heating materials for floor heating and heating textiles.

Acknowledgments. This work was supported by the National Research Foundation of Korea (NRF) Grant funded by the Korean Government (MOE) (2013R1A1A2A10010080).

References

(1) H. Q. Pham, and M. J. Marks, *Epoxy Resins*, in *Kirk-Othmer Encyclopedia of Chemical Technology*, 5th ed., A. Seidel, Ed., John Wiliey & Sons, Hoboken, 2005, Vol. 8, p 347.
(2) D. Ratna and A. K. Banthia, *Macromol. Res.,* **12**, 11 (2004).
(3) *Epoxy Resins, Chemistry and Technology*, C. A. May, Ed., Marcel Dekker, Inc., New York, 1988.
(4) J.-P. Fouassier and J. F. Rabek, *Radiation Curing in Polymer Science and Technology*, Elsevier, London, 1993.
(5) C. Decker, *Prog. Polym. Sci.,* **21**, 593 (1996).
(6) M. Sangermano, R. Bongiovanni, G. Malucelli, and A. Priola, in *Horizons in Polymer Research*, R. K. Bregg, Ed., Nova science publishers Inc., New York, 2006.
(7) S. C. Yang, J. H. Jin, S.-Y. Kwak, and B.-S. Bae, *Macromol. Res.,* **19**, 1166 (2011).
(8) S. Kang, S. I. Hong, C. R. Choe, M. Park, S. Rim, and J. Kim, *Polymer,* **42**, 879 (2001).
(9) M. Fujiwara, K. Kojima, Y. Tanaka, and R. Nomura, *J. Mater. Chem.,* **14**, 1195 (2004).
(10) O. Becker, and G. P. Simon, *Adv. Polym. Sci.,* **179**, 29 (2005).
(11) A. Allaoui and N. El Bounia, *Exp. Polym. Lett.,* **3**, 588 (2009).
(12) M. H. Al-Saleh and U. Sundararaj, *Carbon,* **47**, 1738 (2009).
(13) J. Li, Y. Gao, W. Ma, L. Liu, Z. Zhang, Z. Niu, Y. Ren, X. Zhang, Q. Zeng, H. Dong, D. Zhao, L. Cai, W. Zhou, and S. Xie, *Nanoscale,* **3**, 3731 (2011).
(14) J. G. Park, Q. Cheng, J. Lu, J. Bao, S. Li, Y. Tian, Z. Liang, C. Zhang, and B. Wang, *Carbon,* **50**, 2083 (2012).
(15) S. C. Hong, H. J. Park, J. Y. Chang, and S. S. Lee, *Macromol. Res.,* **20**, 1191 (2012).
(16) M. L. Gupta, S. A. Sydlik, J. M. Schnorr, D. J. Woo, S. Osswald, T. M. Swager, and D. Raghavan, *J. Polym. Sci. Part B: Polym. Phys.,* **51**, 410 (2013).
(17) Y.-K. Choi, K. Sugimoto, S.-M. Song, Y. Gotoh, Y. Ohkoshi, and M. Endo, *Carbon,* **43**, 2199 (2005).
(18) J.-M. Park, D.-S. Kim, S.-J. Kim, P.-G. Kim, D. J. Yoon, and K. L. DeVries, *Compos. Part B,* **38**, 847 (2007).
(19) A. Zhamu, Y. P. Hou, W. H. Zhong, J. J. Stone, J. Li, and C. M. Lukehart, *Polym. Compos.,* **28**, 605 (2007).
(20) Y. Zhou, F. Pervin, and S. Jeelani, *J. Mater. Sci.,* **42**, 7544 (2007).
(21) A. Allaoui, S. V. Hoa, and M. D. Pugh, *Compos. Sci. Technol.,* **68**, 410 (2008).
(22) A. Yasmin, J.-J. Luo, and I. M. Daniel, *Compos. Sci. Technol.*, **66**, 1182 (2006).
(23) S. C. Kim, H.-I. Lee, and H. M. Jeong, *Macromol. Res.,* **18**, 1125 (2010).
(24) S. H. Song, K. H. Park, B. H. Kim, Y. W. Choi, G. H. Jun, D. J. Lee, B.-S. Kong, K.-W. Paik, and S. Jeong, *Adv. Mater.,* **25**, 732 (2013).
(25) L. X. He and S. C. Tjong, *Exp. Polym. Lett.,* **7**, 375 (2013).
(26) J.-E. An and Y. G. Jeong, *Eur. Polym. J.,* **49**, 1322 (2013).
(27) J. Cheng, L. Wang, H. Yu, Q. Yang, and L. Deng, *J. Polym. Sci. Part B: Polym. Phys.,* **46**, 1529 (2008).
(28) C. Brosseau and M. E. Achour, *J. Appl. Phys.,* **105**, 124102 (2009).
(29) X. Ji, H. Li, D. Hui, K.-T. Hsiao, J. Ou, and A. K. T. Lau, *Compos. Part B,* **41**, 25 (2010).
(30) M. El Hasnaoui, J. Belattar, M. E. Achour, L. C. Costa, and F. Lahjomri, *Optoelectron. Adv. Mater. Rapid Commun.,* **6**, 610 (2012).
(31) A. Yu, P. Ramesh, X. Sun, E. Bekyarova, M. E. Itkis, and R. C. Haddon, *Adv. Mater.,* **20**, 4740 (2008).
(32) J. Li, P.-S. Wong, and J.-K. Kim, *Mater. Sci. Eng. A,* **483-484**, 660 (2008).
(33) K. Chu, W. Li, C. Jia, and F. Tang, *Appl. Phys. Lett.,* **101**, 211903 (2012).
(34) S. Chatterjee, F. Nafezarefi, N. H. Tai, L. Schlagenhauf, F. A. Nusech, and B. T. T. Chu, *Carbon,* **50**, 5380 (2012).
(35) W. Li, A. Dichiara, and J. Bai, *Compos. Sci. Technol.,* **74**, 221 (2013).
(36) L. Staudenmaier, *Ber. Dtsch. Bot. Ges.,* **31**, 1481 (1898).
(37) H. C. Schniepp, J.-L. Li, M. J. McAllister, H. Sai, M. Herrera-Alonso, D. H. Adamson, R. K. Prudhomme, R. Car, D. A. Saville, and I. A. Aksay, *J. Phys. Chem. B*, **110**, 8535 (2006).
(38) M. J. McAllister, J.-L. Li, D. H. Adamson, H. C. Schniepp, A. A. Abdala, J. Liu, M. Herrera-Alonso, D. L. Milius, R. Car, R. K. Prudhomme, and I. A. Aksay, *Chem. Mater.,* **19**, 4396 (2007).